

Modelling of Haptic Vibration Textures with Infinite-Impulse-Response Filters

Vijaya L. Guruswamy, Jochen Lang and Won-Sook Lee
School of Information Technology and Engineering
University of Ottawa
Ottawa, Canada ON K1N 6N5
Email: vguru054,jlang,wslee@site.uottwa.ca

Abstract—Vibration feedback models are known to be effective to convey tactile characteristics in virtual environments and they can be rendered with existing haptic devices. In this paper we develop a novel texture model based on a spatial distribution of infinite-impulse-response filters which operate in the time domain. We match the impulse response of the filters to measured acceleration profiles obtained from scanning of real-world objects. We report results on surfaces with varying roughness characteristics including surfaces with stochastic variations and surfaces with regular features. Our novel use of infinite-impulse-response filters allows us to represent multiple frequencies of the response, and to unify the haptic texture model to arbitrary surfaces unlike the conventional rendering method for patterned textures based on a decaying sinusoid. We employ an existing hand-held mobile scanning set-up with a visually-tracked probe, which provides acceleration and force profiles. Our simple capturing devices also removes any need for a robotic manipulator.

Index Terms—Haptic, Vibrotactile, Texture.

I. INTRODUCTION

We experience vibrations during contact with our physical environment. One source of vibrations is stroking a surface as we sense and explore our environment. In this process, we may, e.g., use our fingers, finger nails or a tool to excite a vibration response. The vibrations during a stroke convey information about the surface finish and patterns in the surface structure. The pervasiveness of vibrations has motivated Okamura et al. [1] to propose vibration feedback models for virtual environments. Okamura et al. [1] modeled vibrations during stroking of a surface, during tapping as suggested earlier by Wellman and Howe [2] and during membrane puncture. Since then tapping, e.g., Kuchenbecker et al. [3], and needle insertion [4] have received a great amount of attention but it seems vibrotactile textures have received relatively little further investigation despite the fact that Okamura et al. reported that their subjects perceived vibration-based textures as most realistic. Vibration feedback can also be generated with very simple means [5] and it is used in game controllers, cellphones and mobile devices because of its efficacy.

In the work of Okamura et al. [1], haptic textures are classified as either “general” or “patterned”. General textures are basically stochastic without any discernible features, e.g., sandpaper, while patterned textures have regular distinguishable features, e.g., groves. Okamura et al. fit a decaying

sinusoid to the acceleration profile in the time domain in the case of patterned textures. To the best of our knowledge, they have done no further work for stochastic textures beyond identifying the dominant frequency in the acceleration profile. While we confirm their observation that features cause a decaying impulse-response when stroking the surface, we develop a novel unified filtering method for both, general and patterned surfaces. Instead of a decaying sinusoid to model the acceleration response normal to the surface as a probe is moved across it, we choose to use an infinite-impulse-filter (IIR) to model this response. This allows us to use a higher order filter to capture more than just the dominant frequency of the response as well as to unify the haptic texture model on arbitrary surfaces. In particular, we claim that stochastic textures are simply a collection of many low amplitude impulse responses at high spatial frequency. Our unified model is general for any surface and simple to render with low latency because of the computational simplicity of IIR filters.

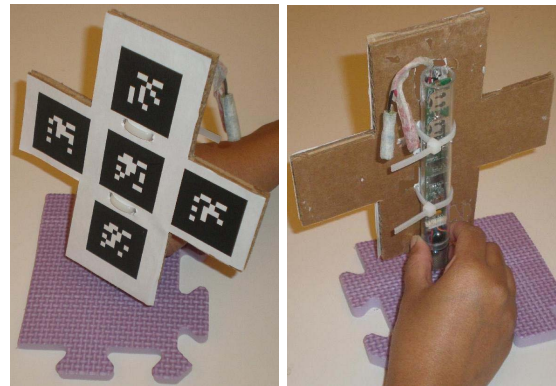


Fig. 1. Scanning with the WHaT.

We estimate our IIR models from force-acceleration profiles collected during stroking of real-world surfaces with a wireless haptic texture sensor, the WHaT [6]. We employ a system initially developed by Andrews and Lang [7] based around the WHaT which is not the subject of this paper but we inherit the advantages of that system. Most important for our current work is the ability to collect force-acceleration profiles from free-

form surfaces without resulting to sampling (see Figure 1), i.e., our models can be estimated from surfaces measured on-site. Otherwise, collecting data from physical environments can be quite tedious and may even prevent the use of reality-based models for virtual environments but we believe that our flexible approach is well-matched to the ease in rendering vibration models and can help to bring more realism to virtual environments.

The remainder of this paper is organized as follows: Section II provides a brief discussion of haptic texturing. We present our IIR-filter-based haptic texture model along with a rendering routine in Section III. Section IV details the estimation of IIR-filter parameters from our measurements, both, for a single feature of a texture and for a complete profile. Section V presents estimated profiles for different types of surfaces. We conclude our paper in Section VI with some future directions.

II. BACKGROUND AND RELATED WORK

Haptic textures are a common part of Virtual Environments and many different modelling and rendering approaches exist. In their sandpaper system, Minsky et al. [8] render forces based on the gradient of the local surface. The surface texture is either represented procedurally or by an image. Since then, many different approaches have been suggested. Siira and Pai [9] use normal variations derived from surface roughness parameters for their stochastic textures. Basdogan et al. [10] model textures as bump maps which are either derived procedurally or from images similar to computer graphics. Wall and Harwin [11] employ Fourier series to represent a spatial frequency response measured during surface profiling while Costa and Cutkosky [12] simulate surface height profiles with fractals. We are motivated to explore vibrotactile textures by Klatzky and Lederman [13] who state that their “findings support the use of vibrotactile cues to roughness in environments in which direct skin contact is precluded”. Commercial pen-like haptic devices do not simulate skin contact and hence our pursuit of vibrotactile textures.

Early work by Wellman and Howe [2] conveyed the stiffness of virtual objects based on measured vibration waveforms during a tapping experiment. Their work demonstrated that high frequency vibrotactile feedback can effectively alter the way objects are perceived in a virtual environment. Okamura et al. [1] extended the vibrotactile model to the acceleration profiles sensed during stroking of a surface. Their model is a decaying sinusoid which is fit in the time-domain to a acceleration profile acquired when passing a groove in the surface. We extend in our work the vibration feedback model to arbitrary surfaces using a more general decaying impulse response represented by an IIR filter. Our model is also closely related to the event-based haptics approach by Kuchenbecker et al. [3] who model the vibrations during tapping by acceleration matching based on measurements. Acceleration matching estimates the transfer function between force and accelerations based on tapping on samples with the stylus of an actual instrumented haptic device. During rendering with the same

stylus-based device the transfer function is used to generate open-loop vibration transients.

We render our vibration texture also with standard stylus-based haptic devices but simpler devices based on a tactor or inertial motor may be effective as well for vibration textures. According to Hayward and MacLean [5] these types of vibrotactile devices are the most common way to render vibrotactile feedback today and can be found in pagers, cellphones and game controllers. Matrix pin displays [14] based on various technologies may also be effective.

III. IIR FILTER MODEL

We designed our haptic texture model based on the force-acceleration profiles which we have observed in scanning surfaces with the WHaT [9]. The WHaT is a stylus-like instrument which records three-dimensional accelerations and the force along its major axis. The values are transmitted via a wireless link to a host PC at about $500Hz$. Simultaneously, we visually track fiducial markers on the pen (see Figure 1) with a stationary camera at about $100Hz$. The system is described in detail in [7] and has several advantages over commercial profilers and vibration testers. Mobile profilers measure surface height variations for roughness determination but typically do not record accelerations while mobile vibration testers are meant to be kept stationary and both types of instruments do not record forces.

Figure 2 shows three different acceleration profiles normal to the surface that resulted from scanning sandpaper, a rubber mat and a CD jewel case. We selected these objects because they are representative of different types of surfaces. A CD jewel case contains regular ridges and groves and these are recognizable in the acceleration profile in Figure 2(a). The rubber mat consists of a pattern of repeating squares which are discernible in the acceleration profile in Figure 2(b) but mixed with a more stochastic pattern. The accelerations when scanning sandpaper in Figure 2(c) are stochastic without any repeatable pattern.

When a surface is scanned with the probe, an acceleration pulse occurs at locations of peaks and dips in the surface. A positive pulse is generated when the probe runs over a peak in the surface, whereas a negative pulse occurs when the probe falls into a dip. Inspired by Okamura et al. [1], we model such a pulse as the initial peak of a decaying vibration wave, i.e., the feature triggers a vibration at a certain location on the surface which then diminishes over time. Okamura et al. used a decaying sinusoid to represent this relation in the time domain as

$$y(t) = Ae^{-bt} \sin \omega t \quad (1)$$

where A , b and $f = \omega/2\pi$ represent the amplitude, the decay rate and the frequency of the waveform, respectively. They applied their model only to surfaces with features (groves). Decaying impulse responses in time are located at feature locations in space. Figure 3 shows a synthetic example of our interpretation such a haptic texture model with the Figure 3(a) depicting a distribution of the filters over the surface.

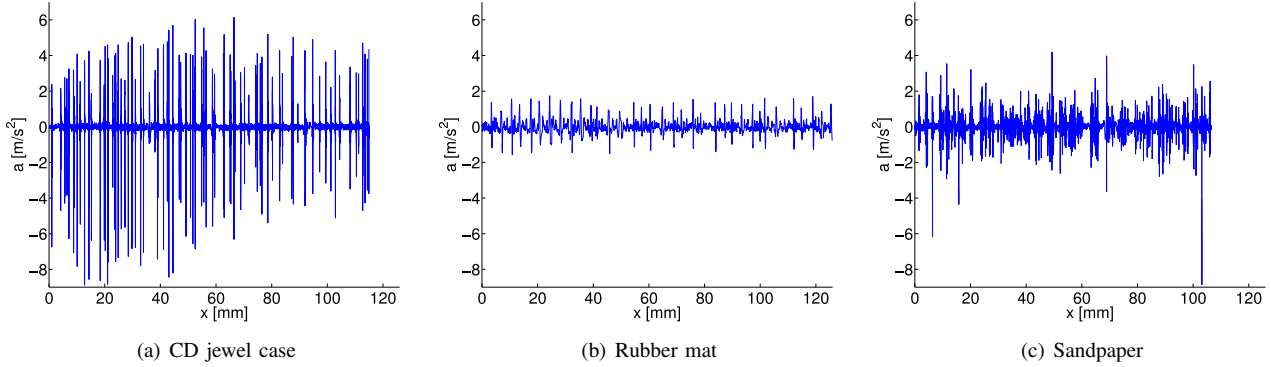


Fig. 2. Measured Acceleration Profiles.

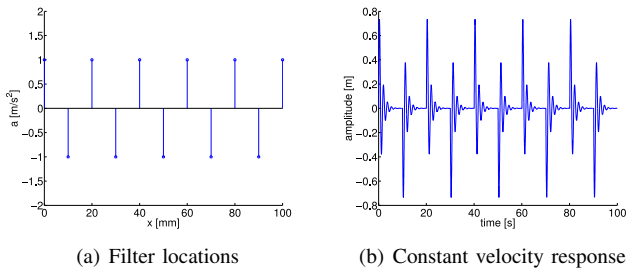


Fig. 3. Haptic texture model with filters due to surface features located in space and damping in time.

Figure 3(b) shows a corresponding acceleration profile if the surface is traversed with constant speed.

We view the decaying sinusoid as the impulse response of a linear shift-invariant system. We model the system with a discrete IIR filter. The filter allows us to generate the vibrations at each feature location by simply inputting an impulse to the filter which then produces the desired vibration pattern in time. Assuming that the vibrations can be described by a decaying sinusoid, then the Z-transform of the IIR filter is given by

$$H(z) = \frac{ze^{-\beta T} \sin(\omega T)}{z^2 - 2ze^{-\beta T} \cos(\omega T) + e^{-2\beta T}} \quad (2)$$

We use a discrete form of the filter with sampling time T since when rendering haptic textures, the impulse response will be created in software. IIR filters have a computational advantage over finite-impulse response filters which is beneficial for haptic rendering.

The most important advantage of the IIR filter model for haptic textures is their ability to have a large range of different frequency responses. We leverage this characteristic of the IIR filter to model richer vibration waveforms based on our measurements of acceleration-force profiles. We design the IIR filter such that its normalized impulse response matches the acceleration profile which we have measured stroking the surface with the WHaT. As a result the IIR filter response to an impulse matches the scaled vibration texture signals. The height of the impulse can be varied based on the force and the speed with which the textured surface is traversed

during haptic rendering. In going beyond the decaying sinusoid model, vibration analysis and modeling will be a more complex task than simply applying Equation 2 and it is the topic of Section IV.

A. Haptic Rendering

For haptic rendering of our texture, we adapt the model of Andrews and Lang [15] in which a point on the triangulated object surface is parametrized as a position along the 1D profile and a distance normal to the profile. The mapping is performed with the help of barycentric coordinates. But instead of rendering a height profile as in [15], we directly use the acceleration profile. Our haptic rendering employs a penalty-based approach where the penalty force is composed of a rigid body constraint force plus a texture force normal to the surface plus a lateral frictional force. We consider the scaled acceleration profile as produced by the IIR filter as the texture force. The texture force is the sum of all K currently active filters. A filter becomes active once the haptic interaction point has traversed the filter location x_k on the profile at discrete time prior to the current sampling time $-t_k = -cT$. The overall normal texture force is then given by

$$F_t(z) = \sum_{k=0}^K A_k z^{-t_k/T} H_k(z)$$

where

$$H_k(z) = \frac{\sum_{i=0}^{M_k} b_{ik} z^{-i}}{\sum_{j=0}^{N_k} a_{jk} z^{-j}}$$

with $M_k \leq N_k$ and $a_{0k} = 1$ for all filters.

We currently render our texture with a stylus-based haptic device with a haptic update rate close to $1kHz$. However, the actual upper frequency which can be felt by the user is much lower due to damping in the device and we are considering to adapt the open-loop rendering method by Kuchenbecker et al. [3].

IV. MODEL ESTIMATION

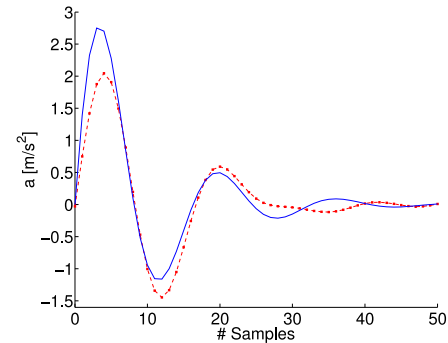
In this section, we discuss the procedure of designing a set of space-sequential IIR filters with a combined impulse response that approximates the acceleration profile over time.

We proceed by segmenting the acceleration profile into sections which have a decaying waveform. We interpret the individual sections as the impulse response from a single filter and find the corresponding IIR filter coefficients with Prony's method [16]. We start our description by considering a single section before introducing our segmentation method. We will illustrate our approach with the acceleration profile from stroking the CD jewel case shown in Figure 2(a).

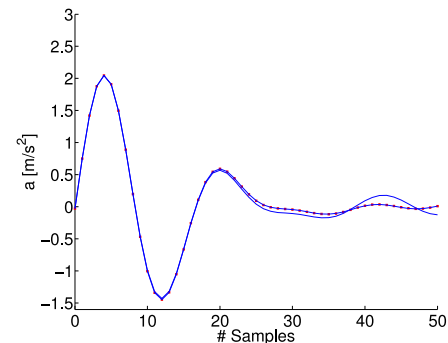
A. Fitting a Segment

Figure 4 shows a section of the acceleration profile in time. The section's start- and endpoint have been selected such that the absolute height of the local extrema are decreasing, i.e., the overall acceleration wave is decaying. Following the method of Okamura et al. [1], we fit a decaying sinusoid to this waveform in the time-domain for comparison. We accomplish the estimation by identifying the dominant frequency of the waveform in the power spectrum of the acceleration profile. The dominant frequency is set as the frequency f of the sinusoid for the decaying sinusoid model of Equation 1. The amplitude A of the wave can be approximated as the height of the first signed peak. We find the decay rate β by fitting an exponential to the absolute heights of the peaks in the segment. The fitted decaying sinusoid corresponds to the model of Okamura et al. for textures with groves but our segments may cover any part of a surface including featureless sections. As discussed earlier, we employ an IIR filter to represent the segment and the decaying sinusoid can be represented as the impulse response of a filter based on equation 2. Figure 4(a) shows the impulse response of the decaying sinusoid filter. While the decaying sinusoid describes the overall nature of the wave, the fit is quite poor.

A closer fitting impulse response can be obtained by higher order IIR filters. We employ Prony's method [16] to design such a filter based on the acceleration data. Prony's method is a time domain method for the calculation of the filter coefficients based on the desired impulse response of the filter. The filter corresponds to a Prony's series which is a sum of damped complex exponentials and hence the series is a natural generalization of the decaying sinusoid model. Prony's method requires a greater number of equidistant samples of the impulse response than the sum of the order plus one of the nominator M and denominator N of the filter. However, higher order filters can be used with the help of zero-padding the impulse response. Figure 4(b) shows two results of Prony's method for the same acceleration profile segment as above. The looser fitting curve was estimated by Prony's method with filter order $M = N = 5$, while for the tighter fit has filter order $M = N = 8$ and is visually not distinguishable from the original samples. In our method, we start with a filter order which equal to the number of extrema of a segment. We increase the order of the filter until the error falls below $0.001m/s^2 = 1.0mm/s^2$. As an error measure we use the sum of absolute differences normalized by the number of samples.



(a) Decaying Sinusoid Model



(b) Prony's Method

Fig. 4. Estimation of IIR filter model. Dots are the measurements, the solid lines are the filter responses. The result of a time domain estimation for a decaying sinusoid is shown in 4(a), the result of Prony's method with $N = M = 5$ and $N = M = 8$, respectively are shown in 4(b). The IIR filter with $N = M = 8$ is the one used in our approach since it is the filter with the smallest number of coefficients for an average absolute sum of acceleration error of less than $1mm/s^2$ and $N = M$.

B. Segmentation

In Section IV-A, we have assumed the existence of a segment of the acceleration profile in time with a decaying wave while defining a segment as a section of the profile where the absolute heights of the local extrema are decreasing. The acceleration profiles (cf. Figure 2) contain however many extrema with a larger absolute magnitude than the earlier extrema. But if the IIR filter is to model the acceleration response to surface features, then the magnitude of its impulse-response should approach zero a short time after the surface feature has been stroked. It is therefore reasonable to assume that each extrema with a larger absolute magnitude than its predecessor is due to a different surface feature from its predecessor. This assumption is also consistent with the decaying sinusoid model. Our segmentation of the profile exploits this assumption and splits the acceleration profile into sections such that the absolute magnitudes of the local extrema are decreasing. Figure 5 shows an example.

We find the local extrema of the absolute value of the acceleration profile. The maxima will be the extrema of the signal and since the acceleration profiles are zero-centered, the minima are the start and end locations of a peak. The

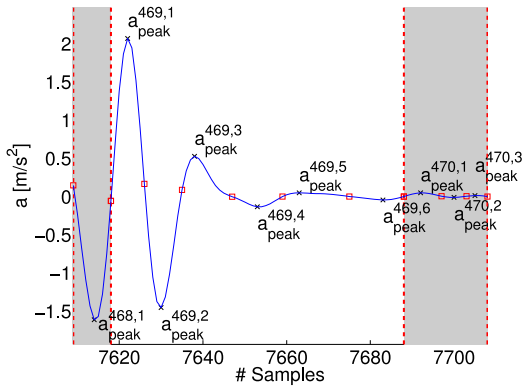


Fig. 5. Segmentation of acceleration profile. The result for segment 469 of the jewel case (see Figure 2(a)) is shown. Note that $|a_{peak}^{i,1}| > |a_{peak}^{i-1,jmax}|$ and that $|a_{peak}^{i,j}| < |a_{peak}^{i,j+1}|$ where i is the i^{th} segment in the profile and j is j^{th} absolute maximum within a segment.

mimima locations determine the length of a segment since each segment extends between the two absolute mimima proceeding the respective sections' absolute maximum (see Figure 5). Searching for extrema in a noisy signal would lead to many false positives and hence it would result in an over-segmentation of the profile. It is therefore necessary to apply a filter first. We employ a bandpass filter with cutoff frequencies selected based on the dominant frequency of the acceleration signal.

V. RESULTS

We present results for the three different raw profiles shown in Figure 2. We would like to emphasize that these results were obtained by a mobile scanning set-up without any requirement for sampling of the surface, i.e., all profiles can be directly obtained by scanning the object. The user follows a free path over the surface, i.e., the profile does not represent a straight line but is registered with the surface of the object through the visual tracker. Details of the registration process can be found in [7]. We would also like to again point out that our results show three different types of profiles ranging from regular patterned to a stochastic profile.

As discussed in Section IV-B, we first employ a bandpass filter to the raw acceleration profiles. The bandpass filter is a 5th-order Butterworth filter and the cutoff frequencies are shown in Table I. We segment the acceleration profile in space to find the location of features and fit the acceleration profile in time as described in Section IV. The IIR filters obtained with Prony's method have varying degree depending on the number of extrema per segment and the quality of fit (see Section IV-B). The result for the CD jewel case is shown in Figure 6(a). The sum of squared errors of the fit compared to the band-pass filtered profile is low as shown in Table I. The number of segments for the CD jewel case is high because the number of samples is high, higher than for the other profiles due to a lower scanning speed, but also because the acceleration profile has more high frequency content.

TABLE I
RESULTS FOR THE ESTIMATION OF THE IIR FILTER MODEL.

Surface	f_{min}	f_{max}	Segment #	$\bar{M} + 1 = \bar{N} + 1$	\overline{SAD} [mm/s^2]
Jewel-case	0.0775	0.1683	1696	5.004	0.0643
Sandpaper	0	0.0980	311	7.170	0.3938
Rubber mat	0	0.1340	242	9.666	0.4299

We use the same procedure to obtain the IIR filters for the sandpaper and the rubber mat profile. The only difference is the frequencies used for the band-pass filter. The frequencies along with the errors of fit for the sandpaper and the rubber mat are shown in Table I and the fitted profiles are shown in Figure 6(c) and Figure 6(b), respectively. Our approach succeeds for all three of the profiles shown in Figure 6 independent of their characteristics, nevertheless, some sources of error exist. The acceleration signal contains frequencies outside the dominant band which may add extra realism to the haptic texture model. If desired, our procedure can be re-iterated with the next minor frequency if the signal for the major frequency is first subtracted from the original signal. A more difficult problem is the time-aliasing which is encountered during scanning. Time aliasing occurs if one decaying wave has not significantly diminished before the next feature is encountered. Our current procedure will simply truncate the earlier decay and add the remaining signal to the new wave. This is not visible if the user's speed during scanning and rendering are well matched but may lead to potential errors, especially, if the motions during rendering are slower than the ones during scanning. Figure 7 shows the haptic texture model for the rubber mat traversed with various constant velocities. We render all of these results with a sampling frequency of $1kHz$. A velocity of $100mm/s$, $1mm/s$ and $0.1mm/s$ is employed for Figures 7(a), 7(b) and 7(c), respectively. The resulting acceleration profiles still look very reasonable despite the fact that velocities of $1mm/s$ and $0.1mm/s$ are much slower than the (non-uniform) scanning speed (cf. with Figure 6(b)).

While we vary the amplitude of the acceleration profile depending on the user force, we do not take into account that Okamura et al. found that the amplitude also depends on the scanning velocity. This issue could be addressed by scanning the same surface multiple times and estimating the velocity based on the position data from the visual tracker. So far, we have not observed any dependency on velocity but this may be due to the fact that with our human-in-the-loop scanning system, the velocities do not vary widely.

VI. CONCLUSION

In this paper we develop a novel method to obtain vibrotactile textures from real-world samples. Our novel texture model consists of spatially distributed and computationally efficient IIR filters which operate in the time-domain. During haptic rendering of the profiles, the user can traverse the textured

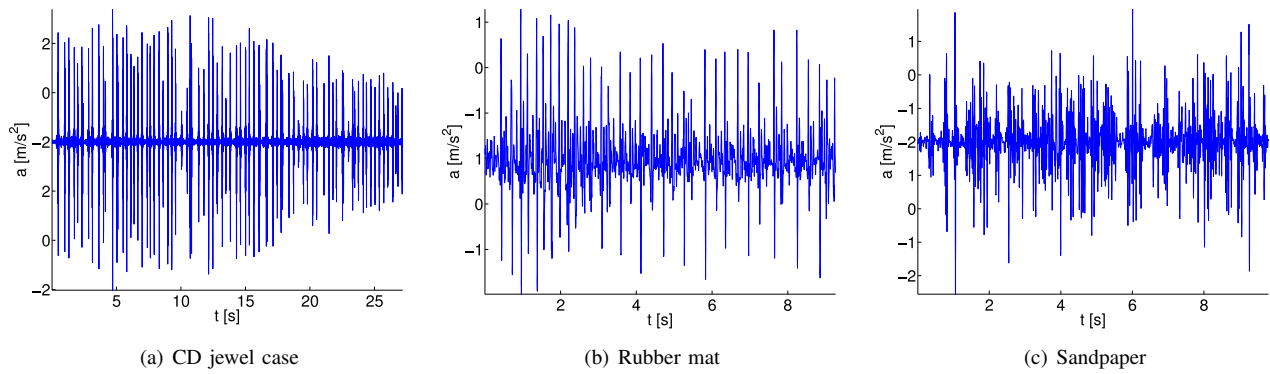


Fig. 6. Haptic textures rendered with the IIR filter model. There is no perceivable error if rendering speed is equal to scanning speed. See also Table I

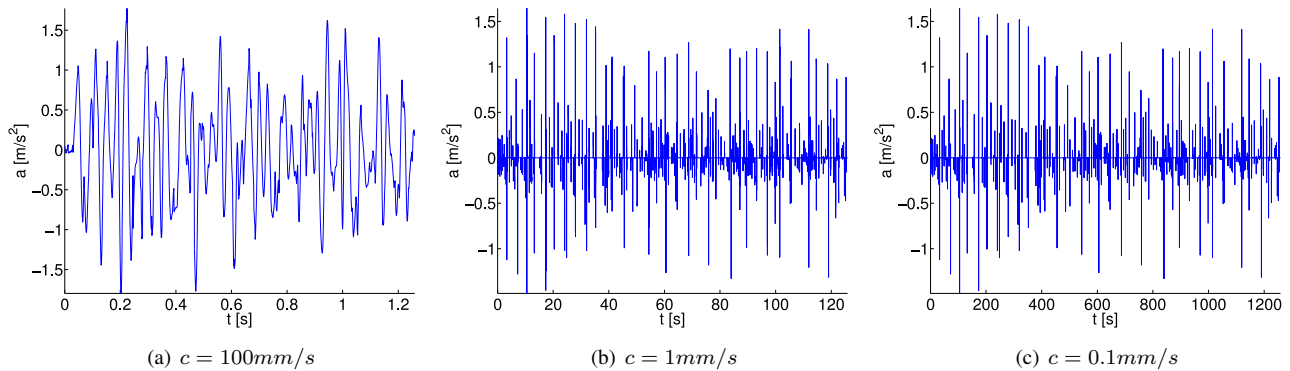


Fig. 7. Haptic textures for the rubber mat rendered with constant force and various constant velocities.

surface at any speed and the spatial frequencies of the features remain constant but the damping is dependent on the velocity. Our procedure extends and unifies the decaying sinusoid approach which has been proposed by others previously. Our estimation method is able to estimate suitable IIR filters for stochastic, patterned and mixed surfaces. The method is based on a segmentation and the use of Prony's method for filter design. In future work, we would like to study the variance introduced into the estimated textures from scanning variations, in particular, due to scanning speed.

ACKNOWLEDGEMENT

The authors gratefully acknowledge the financial support from the Natural Sciences and Engineering Research Council of Canada (NSERC).

REFERENCES

- [1] A. Okamura, J. Dennerlein, and R. Howe, "Vibration feedback models for virtual environments," in *Proc. IEEE Intl. Conf. Robotics and Automation*, 1998, pp. 674–679.
- [2] P. Wellman and R. Howe, "Towards realistic vibrotactile display in virtual environments," *ASME Dynamic Systems and Control Division*, vol. 57, no. 2, pp. 713–718, 1995.
- [3] K. Kuchenbecker, J. Fiene, and G. Niemeyer, "Improving contact realism through event-based haptic feedback," *IEEE Transactions on Visualization and Computer Graphics*, vol. 12, no. 2, pp. 219–230, 2006.
- [4] N. Abolhassani, R. Patel, and M. Moallem, "Needle insertion into soft tissue: A survey," *Medical Engineering & Physics*, vol. 29, no. 4, pp. 413–431, 2007.
- [5] V. Hayward and K. Maclean, "Do it yourself haptics: part I," *IEEE Robotics & Automation Magazine*, vol. 14, no. 4, pp. 88–104, 2007.
- [6] D. Pai and P. Rizun, "The WHaT: A wireless haptic texture sensor," in *Proc. 11th Symp. on Haptic Interfaces for Virtual Environment and Teleoperator Systems*, Los Angeles, USA, 2003.
- [7] S. Andrews and J. Lang, "Interactive scanning of haptic textures and surface compliance," in *Proc. 6th Int. Conf. on 3-D Digital Imaging and Modeling*, Aug. 2007, pp. 99–106.
- [8] M. Minsky, O.-Y. Ming, O. Steele, J. F.P. Brooks, and M. Behensky, "Feeling and seeing: issues in force display," in *Proc. Symp. on Interactive 3D Graphics*. ACM Press, 1990, pp. 235–241.
- [9] J. Siira and D. Pai, "Haptic rendering: A stochastic approach," in *Proc. 1996 IEEE Intl. Conference Robotics and Automation*, 1996, pp. 557–562.
- [10] C. Basdogan, C. Ho, and M. Srivasan, "A ray-based haptic rendering technique for displaying shape and texture of 3d objects in virtual environment," in *Proc. Of the ASME Dynamic Systems and Control Division*, 1997, pp. 77–84.
- [11] S. Wall and W. Harwin, "Modelling of surface identifying characteristics using fourier series," in *Proc. Symp. on Haptic Interfaces for Virtual Environments and Teleoperators*, 1999, pp. 65–71.
- [12] M. Costa and M. Cutkosky, "Roughness perception of haptically displayed fractal surfaces," *Proc. of the ASME Dynamic Systems and Control Division*, vol. 69, no. 2, pp. 1073–1079, 2000.
- [13] R. Klatzky and S. Lederman, "Tactile roughness perception with a rigid link interposed between skin and surface," *Perception & Psychophysics*, vol. 61, no. 4, pp. 591–607, 1999.
- [14] M. Hafez, "Tactile interfaces: technologies, applications and challenges," *Vsual Computer*, vol. 23, no. 4, pp. 267–272, 2007.
- [15] S. Andrews and J. Lang, "Haptic texturing based on real-world samples," in *Proc. IEEE Int. Workshop on Haptic Audio Visual Environments and their Applications: HAVE*, October 2007.
- [16] T. Parks and C. Burrus, *Digital Filter Design*. John Wiley & Sons, 1987.